JOURNAL OF Materials CHEMISTRY

Magnetic properties of two-dimensional triangular arrays of Ni ions in nickel phyllosilicates

M. Richard-Plouet and S. Vilminot

Institut de Physique et Chimie des Materiaux de Strasbourg, Groupe des Matériaux Inorganiques, CNRS-ULP-ECPM-UMR 046, 23 rue du Loess, Strasbourg 67037, France

Synthetic phyllosilicates, with nickel replacing the magnesium atoms, have been prepared under autogenous pressures at 220 °C. Both 1 : 1 phyllosilicate, having interlayer spacing of 7 Å, and 2 : 1 phyllosilicate with 9.4 Å spacing were obtained depending on the metal to silicon ratio. The latter was also expanded to 13.2 Å by use of an amine substituted silicon alkoxide. Dissolution of the silicate precursors was achieved in the presence of fluoride as NH_4F or HF. The microcrystalline products were characterised by X-ray diffraction, thermal analysis, transmission microscopy and chemical analyses. All the samples show long range ferromagnetic order below 28 K accompanied by a rounded maximum in the specific heat measurements. At 4 K they show hysteresis in the magnetisation, with a remnant value ranging from 0.8 to 1.5 μ_B depending on orientation of the applied field and coercive fields up to 3240 Oe.

There has been much interest in the search for low-dimensional magnetic materials in the last twenty years. Several guidelines for obtaining ordered magnetic materials based on theory have been described. On a practical side, there are numerous approaches in the development of new and interesting materials. On the one hand, there exists a school of chemists who devise novel systems through the synthesis of ligands which have the ability to organise transition metal atoms in certain orientations.[1–5] On the other hand others make use of existing structures and introduce magnetic centres that will promote magnetic interactions. We have adopted the latter approach in the present study and have utilised the phyllosilicate framework as the basis for the structure. Among the numerous natural phyllosilicates, we have chosen $Mg_3Si_2O_5(OH)_4$ and $Mg_3Si_4O_{10}(OH)_2$ in which Mg is replaced by nickel ($S=1$) and cobalt ($S=3/2$) as spin centres. When the metal(II) to silicon ratio (M/Si) is 3/2, one layer consists of linking one tetrahedral Si sheet with one octahedral M sheet, giving rise to a 1 : 1 phyllosilicate. The *c* parameter and thus the distance between two adjacent metal sheets, is close to 7 Å. When M/Si = 3/4, two silicate sheets interleave the inner metal sheet, the interlayer distance is thus close to 9.4 Å in this 2 : 1 phyllosilicate. 1 : 1 and 2 : 1 phyllosilicates present the same two-dimensional triangular array of metal ions. These systems complement the one-dimensional compounds, $M^{II}(ReO_4)_2$ (M = Ni, Fe and Co)[6] where transition to a long range ferromagnetic order has been observed. The present study aims at developing two-dimensional arrays.

To our knowledge there are few ferromagnetic materials based on nickel. Only one study to investigate magnetic properties of these silicates is known.[7] We have reproduced the latter and modified the method of synthesis. The present work deals with three nickel compounds. The materials prepared by a hydrothermal method present, as expected, ferromagnetic transitions at higher temperature than for the one-dimensional system mentioned above. Here, we present the synthesis, molecular characterisation and the magnetic properties as a function of temperature and magnetic field. We propose that these materials may be used as a novel system for intercalation with organic molecules in order to tune the magnetic interaction between planes.

Experimental

Synthesis

All reactions were performed in autoclaves under autogenous pressure at 220 °C, using stainless steel bombs with a PTFE lining. The experimental conditions for the preparation of the precursor suspensions are gathered in Table 1. The suspensions were poured in the 125 ml sealed reactor and heated at 220 °C. The reaction times are different from one sample to another: 141 h for sample 1 and 162 h for samples 2 and 3. At the end of the reaction, the bombs were quenched to room temperature by immersion in cold water. The solids were retrieved by filtration, subsequently washed with water and acetone and dried in air.

Two processes could lead to the synthesis of sample 1

Table 1 Experimental conditions concerning the precursor suspensions. The numbers correspond to the mole numbers of the reaction

	sample 1 1 : 1 phyllosilicate	sample 2 2 : 1 phyllosilicate	sample 3 2 : 1 phyllosilicate
$Ni(CH_3COO)_2{\cdot}4H_2O$	3	3	3
H_2O	170	213	31
silica	2 TEOS[a]	4 TEOS[a]	2 TEOS + 2 TAOS[b]
ethanol	0	0	31
NH_4F	1	1	1

[a]The silica precursor, tetraethylorthosilicate (TEOS), is hydrolyzed and condensed to a gel. This was partly dried at 95 °C for 30 min and then ground and dispersed in $Ni(CH_3COO)_2$–NH_4F aqueous solution. [b]Half of the TEOS is replaced by *N*-(2-aminoethyl)-3-aminopropyltrimethoxysilane [$H_2N(CH_2)_2NH(CH_2)_3Si(OCH_3)_3$, TAOS]. This was hydrolyzed and condensed to a gel with ethanol, the hydration water coming from $Ni(CH_3COO)_2$ and HF. Ethanol, TEOS and NH_4F were added to this blue gel.

(Ni/Si = 3/2) as depicted in Fig. 1. In order to improve crystallisation, fluoride was added to the suspensions. The main difference between the two routes is that, in the first case, the gel is dried prior to mixing with the nickel acetate and ammonium fluoride solution, a colloidal suspension being used as precursor. In the second case, the nickel acetate solution is mixed with the gel, a 'gel suspension' being then the precursor. In both cases, the silica gel was obtained by acid catalysed hydrolysis (a few drops of HF) of TEOS [tetraethylorthosilicate, $Si(OC_2H_5)_4$]. Identical results were obtained with either procedure. In the case of the colloidal suspension, no influence of the Ni concentration in solution or of the fluoride source, HF or NH_4F, was observed.

The so-obtained powder is light green with chemical analysis (mass%): 70.62, Ni, 22.52 Si, 6.86 F (percentages do not take into account the oxygen content.)

The first procedure was used to prepare sample 2 (Ni/Si = 3/4). A pure phase of this sample can be obtained from 7.777 g nickel acetate, 0.385 g NH_4F, 8.670 g TEOS and 40 ml H_2O. However, the process appears less flexible than for sample 1. Varying the H_2O quantities and/or the source or quantities of fluoride often leads to a mixture of samples 1 and 2. Synthesis using the second process always promotes the formation of a less crystallised compound.

The powder is also light green and has the following chemical analysis (mass%): 59.49 Ni, 37.94 Si, 2.57 F.

Sample 3 was obtained by replacing half of TEOS by an amine modified alkoxide, *N*-(2-aminoethyl)-3-aminopropyltrimethoxysilane [$H_2N(CH_2)_2NH(CH_2)_3Si(OCH_3)_3$, TAOS]. The latter was first hydrolysed and condensed into a gel in ethanol with several drops of HF with hydration water coming from nickel acetate. To the so-obtained blue gel was added ethanol, TEOS and NH_4F. The colour of the powder was slightly different from the previous two samples and is a darker green with chemical analysis (mass%): 58.11 Ni, 37.07 Si, 2.50 F, 2.31 N.

Characterisation

Air-dried products were examined by X-ray diffraction (XRD) on a Siemens D5000 diffractometer in a Bragg–Brentano geometry using Cu-Kα_1 radiation ($\lambda = 1.5406$ Å).

Thermogravimetry (TG) and differential thermal (DTA) analyses were performed, under air or argon, on a Setaram TGA 92 apparatus, using heating rate of 6 °C min^{-1}. A mass spectrometer was used to obtain information about the evolved compounds during heating.

For electron microscopy, samples were dispersed in ethanol and then collected on a carbon film, which was previously deposited on a copper grid. Observations were performed on a Topcon 002B microscope operating at an accelerating voltage of 200 kV.

Magnetic susceptibilities were recorded from powder samples using Manics Faraday-type equipment in the range 4–300 K.

Isothermal magnetisation data were obtained using a Foner type vibrating sample magnetometer allowing measurements at different temperatures in applied magnetic fields up to 17 000 Oe. The evolution of remnant magnetisation with temperature was also measured. Samples were cooled to 4 K, a magnetic field applied and magnetisation was recorded while the temperature was increased. In order to take into account possible magnetic anisotropy due to the lamellar structure, magnetisation experiments were performed on pellets (*ca.* 5 mm diameter and 2 mm thickness). It was confirmed by XRD that preferential orientation of the crystallites took place. The (00*l*) planes are roughly collinear to the section of the pellets. The magnetic field was applied both perpendicular and parallel to the pellet section, *i.e.* along the same directions with respect to the structure layers.

Specific heat measurements were performed using a quasi-adiabatic calorimeter, between 1.5 and 40 K.

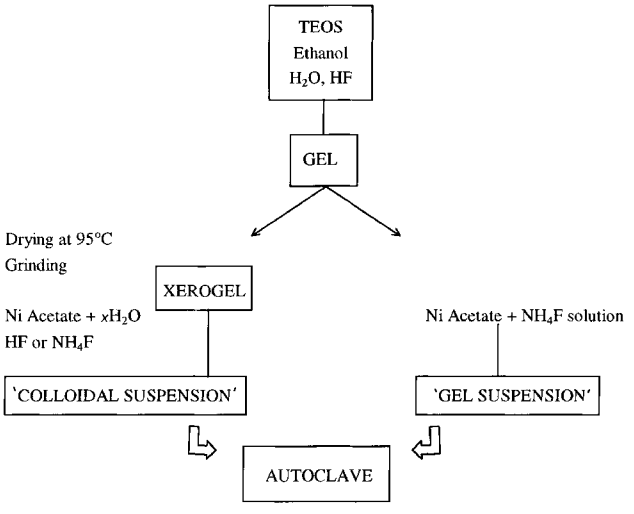

Fig. 1 Schematic description of the experimental procedures used for the synthesis

Results and Discussion

Diffraction and structure

XRD patterns for the three samples are displayed in Fig. 2. In general the diffraction peaks are relatively broad as usually observed for synthetic phyllosilicates. Sample 1 presents, as expected, an XRD pattern and an interlayer spacing characteristic of a 1:1 phyllosilicate. For comparison, the diffraction lines of a natural 1:1 phyllosilicate [$Mg_3Si_2O_5(OH)_4$] are also shown, according to JCPDS file 22-1160. The ideal structure of a 1:1 phyllosilicate is built up by corner-sharing SiO_4 tetrahedra and edge-sharing NiO_6 octahedra linked sheets, as depicted in Fig. 3(*a*) and (*b*). The metal atoms are thus arranged in triangular planes and two types of magnetic interactions occur between them. One is direct while the other is indirect *via* oxygen or hydroxide links at 90°. The NiO_6 sheets are 7 Å apart, as deduced from the position of the first diffraction peak which is associated with the (001) lattice plane. First attempts to enhance the interlayer distance, by using an amine modified alkoxide, *N*-(2-aminoethyl)-3-aminopropyltrimethoxysilane (TAOS) instead of TEOS, led to the formation of a mixture of Ni and of a 13.4 Å phyllosilicate. The XRD patterns of samples 2 and 3 are typical of 2:1 phyllosilicates and the interlayer spacing is *ca.* 9 Å. XRD peaks of $Mg_3Si_4O_{10}(OH)_2$ (talc) (JCPDS file 29-1493) are also shown in Fig. 2. The layers are

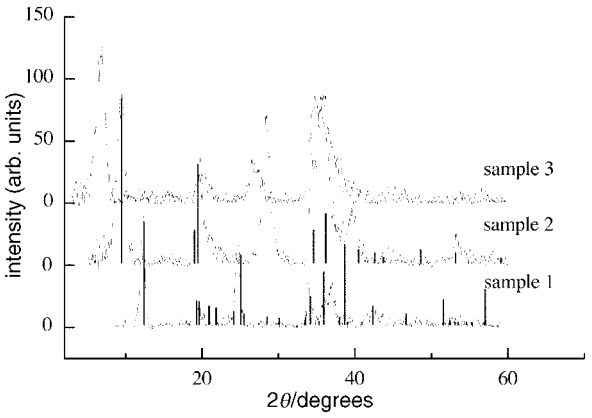

Fig. 2 XRD patterns of samples 1, 2 and 3 ($\lambda = 1.5406$ Å)

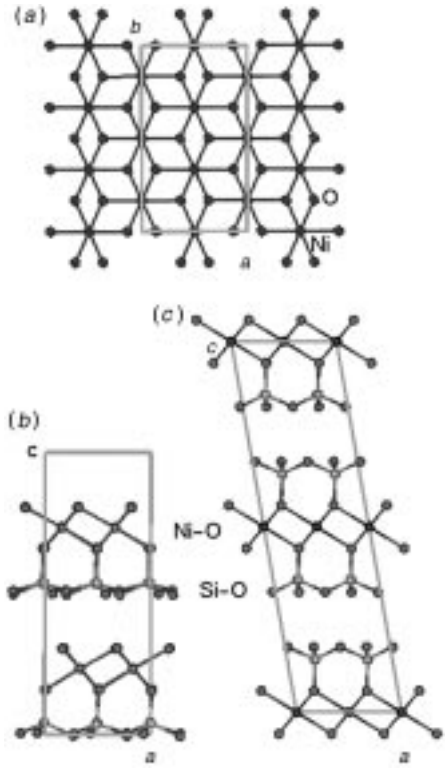

Fig. 3 (*a*) Representation of Ni environment in the *a*,*b* plane; (*b*) ideal 1:1 phyllosilicate structure;[4] (*c*) ideal 2:1 phyllosilicate structure[5]

built up of one sheet of nickel atoms in octahedral coordination between two SiO_4 sheets [Fig. 3(*c*)].

Sample 2 which was prepared by employing TEOS as the Si precursor corresponds to a talc-like structure with a distance between Ni sheets close to 9.4 Å whereas for sample 3 obtained using TAOS this distance is larger and close to 13.2 Å. Attempts to enhance the interlayer distance by using a longer modifying agent [*N*-(6-aminohexyl)-3-aminopropyltrimethoxysilane] led to a 13.3 Å expanded 2:1 phyllosilicate.

Microscopy

TEM observations reveal that sample 1 exhibits lamellar crystallites, with dimensions of *ca.* 20 nm. Sample 2 presents two kinds of crystallites: some with a diameter close to 500 nm and the others with a diameter of 10 nm. For sample 3, the crystallites have a ribbon-like shape with a thickness close to 10 nm and length 50–100 nm. Some characteristic features of the morphologies are illustrated in Fig. 4.

Thermogravimetry and thermal analysis

For the three samples, characteristic features can be distinguished on the TG curves (Fig. 5). The first mass loss below 200 °C, associated with a broad endothermic effect, is related to removal of adsorbed species, mainly H_2O and constant mass is achieved at 1300 °C. The XRD diagram of the final product is characteristic of a mixture of Ni_2SiO_4 and SiO_2.

Sample 1 presents a second mass loss between *ca.* 500 and 690 °C, corresponding to the dehydroxylation of the silicate, as confirmed by the loss of H_2O observed by mass spectrometry and corresponding to the endotherm whose minimum is at *ca.* 620 °C. The last mass loss in the 1100–1200 °C region corresponds to sample defluorination as revealed by mass spectrometry.

Sample 2 reveals a similar thermal evolution even if the dehydroxylation temperature is quite different from that of sample 1. In the latter case, H_2O evolution takes place between 900 and 1120 °C (corresponding endotherm minimum at

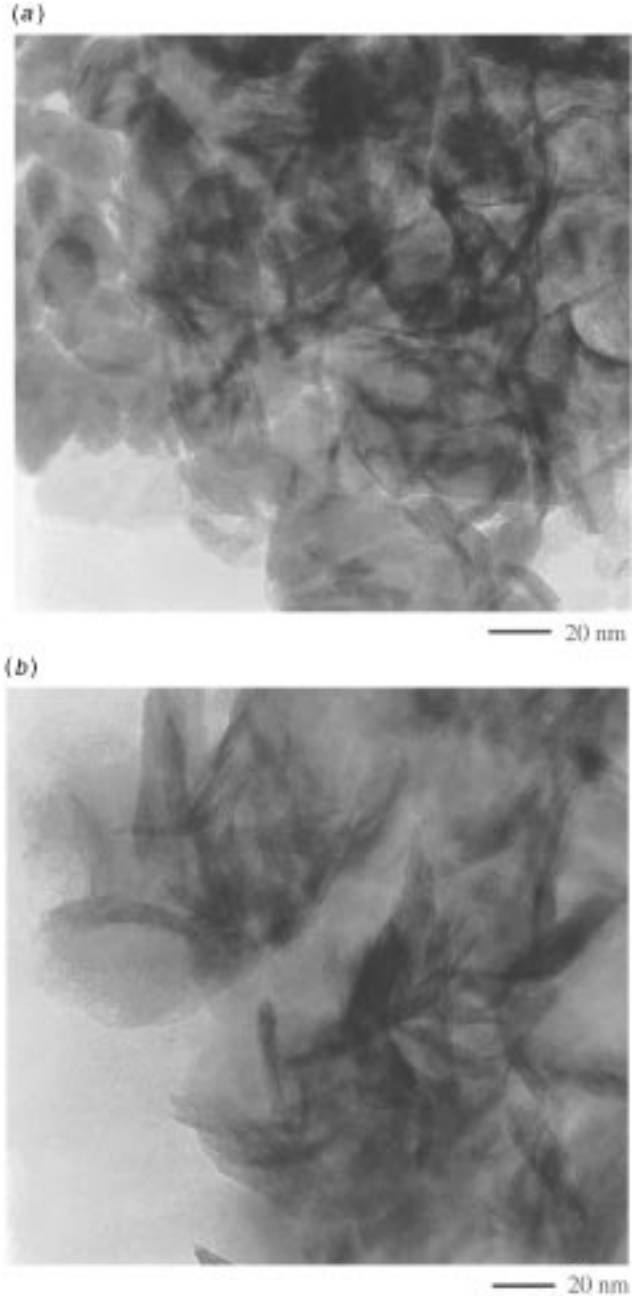

Fig. 4 Transmission electron microscopy images: (*a*) sample 1, (*b*) sample 3

990 °C) and is immediately followed by the defluorination process. Moreover, the larger mass loss for the 1:1 compared to the 2:1 sample is expected according to the corresponding reactions:

1:1 phyllosilicate: $Ni_3Si_2O_5(OH)_{4-x}F_x \rightarrow$

$$3\ NiO + 2\ SiO_2 + (4-x)/2\ H_2O + x\ F$$

2:1 phyllosilicate: $Ni_3Si_4O_{10}(OH)_{2-x}F_x \rightarrow$

$$3\ NiO + 4\ SiO_2 + (2-x)/2\ H_2O + x\ F$$

It should be mentioned that these reactions are only global and that they do not take into account the possible reactions between products.

The situation is quite different for sample 3 which is characterised by a strong exotherm peaking at 400 °C on the DTA trace, associated with a mass loss larger than for the other samples. This is related to the presence of amine groups inside the structure since it is prepared in the presence of TAOS. The strong exotherm indicates the combustion of amine groups.

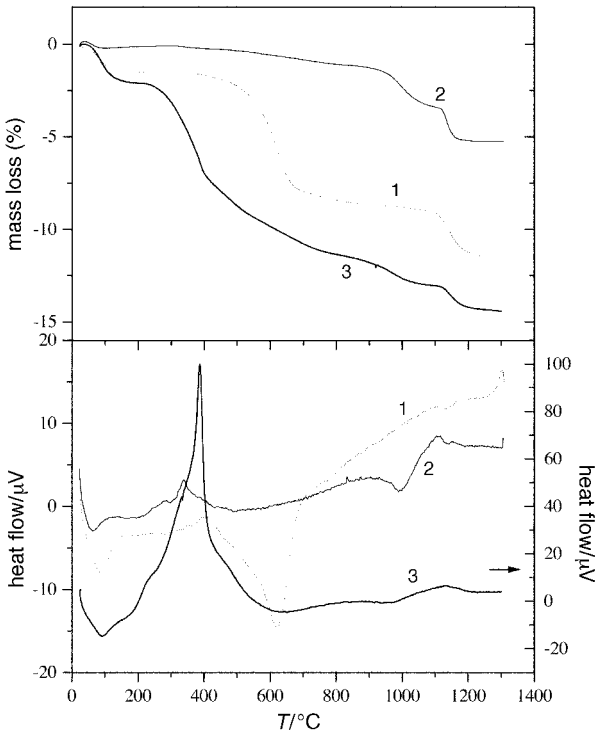

Fig. 5 TG and DTA curves for samples 1, 2 and 3. The experiments were performed under air atmosphere.

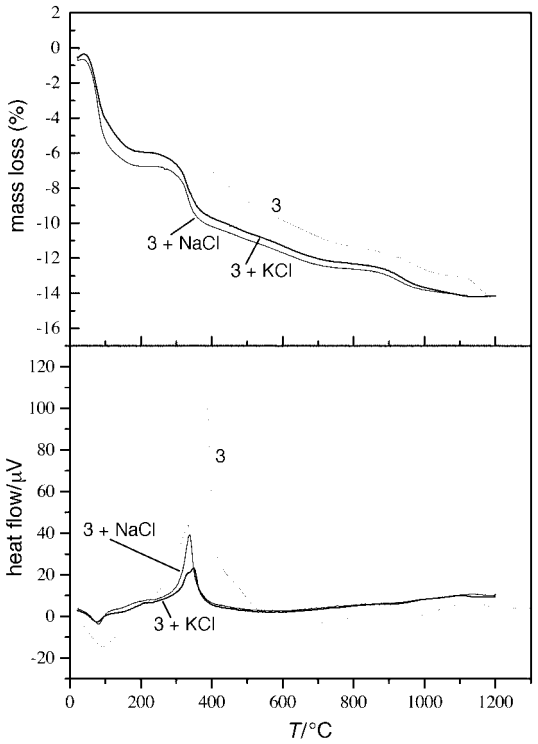

Fig. 6 TG and DTA curves for sample 3 treated with NaCl and KCl. The experiments were performed under air atmosphere.

The XRD pattern of samples heated to 800 °C is characteristic of a talc-like 2 : 1 phyllosilicate ($d_{001} = 9.5$ Å). At higher temperature, the dehydroxylation and defluorination steps are observed and confirmed by mass spectrometry, although the first process is much less clear.

For samples 1 and 2, a small exotherm is also observed below 400 °C, with formation of CO_2 but its origin is unknown. As only TEOS was used, it cannot have the same origin as for sample 3. This phenomenon was not observed under argon atmosphere, nor was it observed when silica prepared by atomisation, instead of TEOS, was used as the Si precursor.[10] Therefore, this could be related to the combustion of some organic residues arising from alkoxide. To elucidate the origin of this transformation IR spectra were measured on samples which were heated to just before and after this exothermic peak; however, no significant changes in the vibrational bands could be detected.

If thermal analysis were able to detect the presence of fluoride in the samples in a manner similar to the observation of the amine groups in sample 3, it would not allow the determination of the corresponding formulations. The stoichiometry of our compounds was determined from chemical analyses performed at the Service d'Analyse du CNRS in Vernaison. From chemical analysis of the Ni/Si ratio and the substitution ratio of OH^- by F^- the following formulations were obtained.

sample 1: $Ni_3Si_2O_5(OH)_{3.1}F_{0.9}$

sample 2: $Ni_3Si_4O_{10}(OH)_{1.6}F_{0.4}$

sample 3:

$$Ni_3Si_4O_{10-x}(OH)_{1.6}F_{0.4} \cdot x[(CH_2)_3NH(CH_2)_2NH_2] \quad (0.2 \leqslant x \leqslant 0.3)$$

The fluoride and hydroxide contents are consistent with the mass losses observed in TG.

Further experiments were performed to find out whether the amine group is exchangeable or not. Sample 3 was stirred in 1 M NaCl or KCl aqueous solutions for 4 days. The powders were retrieved by filtration, washed with water to eliminate excess chloride and finally washed with acetone before drying in air. The XRD patterns of the resulting samples exhibit a similar pattern to that of the initial phyllosilicate structure. The crystallinity, however, appears to be lower than before treatment with a broadening of the diffraction lines. However, the (001) diffraction line corresponds to a slightly different interlayer separation: from 13.2 Å to 13.5 and 13 Å for Na^+ and K^+ treated samples, respectively. The corresponding TG–DTA traces reveal some features similar to sample 3 (Fig. 6) with a first mass loss below 200 °C, associated with an endothermic effect, and a strong exotherm between 300 and 400 °C. The first mass loss is much larger for both treated samples compared to untreated sample 3. XRD measurements performed on samples annealed at 250 °C do not reveal any modification. It therefore seems reasonable to consider that the first mass loss and endotherm is related to removal of adsorbed water, as for sample 3. Considering now the strong exotherm, its maximum occurs at a lower temperature (340 °C) for treated samples than for untreated sample 3 (390 °C). The same shift is also observed for the endothermic effect recorded on DTA traces under argon atmosphere with minimum temperatures of 395 and 440 °C for treated and untreated samples, respectively. In all cases, a mixture of Ni_2SiO_4 and SiO_2 is evidenced by XRD as the final product. With the hypothesis that the first mass loss corresponds to water desorption a smaller mass loss is observed between 200 and 1200 °C, for treated samples, (7.5, 8.3% for Na^+, K^+ samples *cf.* 12.3% for sample 3). Therefore, all these differences seem to indicate that some exchange reactions have taken place.

Magnetic properties

Consistent with the previous magnetic studies, all our samples show long range ferromagnetic order below 28 K.[7,11] The temperature dependence of the magnetic susceptibilities in a field of 12000 Oe are shown in Fig. 7. They are strongly dependent on the applied magnetic field at low temperatures suggesting non-linear magnetisation. The susceptibility curves can be fitted to the Curie–Weiss law, between 100 and 300 K, giving the following results: C(emu K/mol Ni) = 1.2, 1.0 and

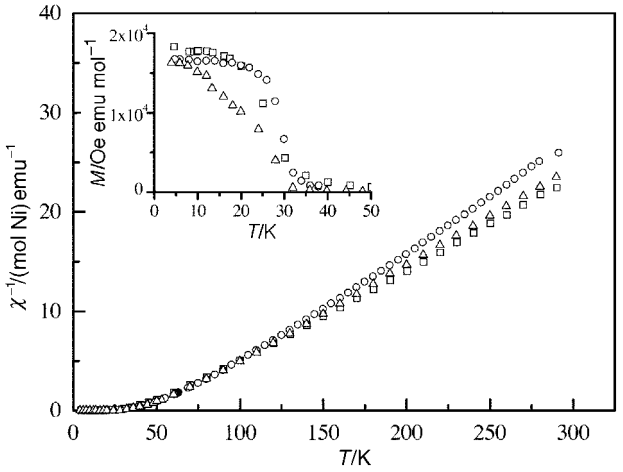

Fig. 7 Temperature dependence of the magnetic susceptibility for samples 1 (□), 2 (○) and 3 (△)

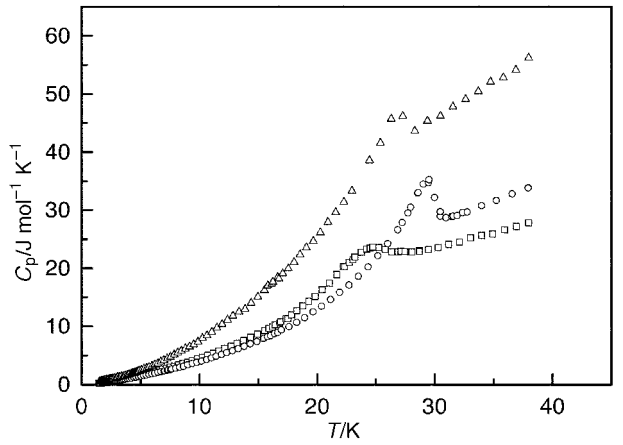

Fig. 8 Temperature dependence of the specific heat capacity for samples 1 (□), 2 (○) and 3 (△)

Table 2 Curie temperatures determined from specific heat and remnant magnetisation measurements

	sample 1	sample 2	sample 3
T_C (C_p)/K	25	29	27
T_C (M_{rem})^a/K	26	25	27.5
T_C (M_{rem})^b/K	27	28.5	28

^{a}Perpendicular to the applied field direction. ^{b}Parallel to the applied field direction.

1.1 for and θ(K) = 47.1, 57.4 and 50.5 for samples 1, 2 and 3, respectively. As expected for ferromagnetic materials, the Weiss constants are positive and higher than the transition temperatures. In the paramagnetic region, the g values are found to be 2.2, 2.0, 2.1 for samples 1, 2 and 3, respectively. The calculation was performed using a spin only equation $C = Ng^2\mu_B{}^2S(S+1)/3k$ with $S=1$ for Ni^{2+}. These are in good agreement with those expected for octahedral nickel(II) which lies between 2.0 and 2.5.

The results of specific heat measurements are plotted in the temperature range 1.5–40 K in Fig. 8. They show the presence of broad peaks associated with the para–ferromagnetic transition, temperatures of which are listed in Table 2.

The transition temperatures have also been estimated from the temperature evolution of the remnant magnetisation as depicted in Fig. 9 for two applied field directions. In both cases, the corresponding curves have a similar shape, showing two steps that are clearly visible in the case of sample 2, and especially when the applied field direction is perpendicular to

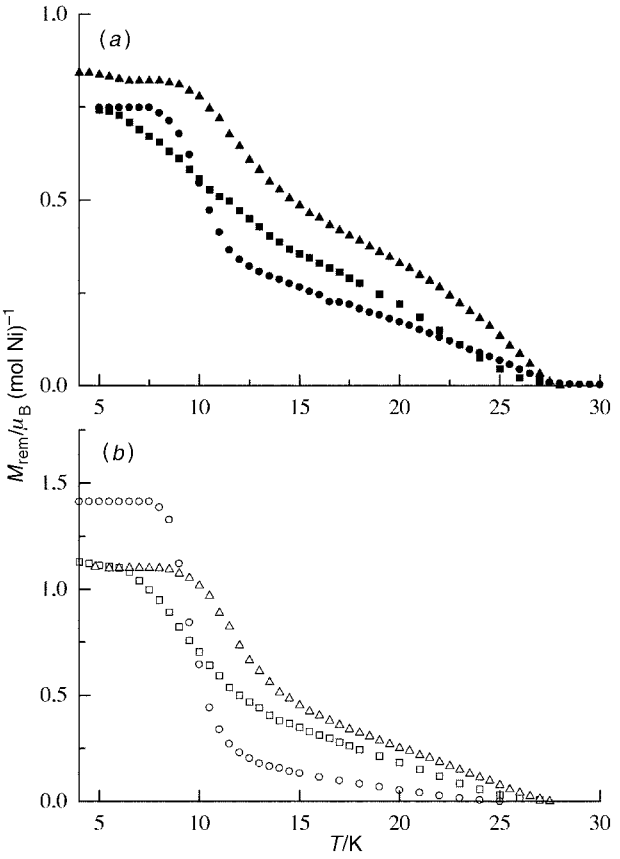

Fig. 9 Remnant magnetisation curves for (*a*) H parallel and (*b*) H perpendicular to the layers of the structure for samples 1 (■, □), 2 (●, ○) and 3 (▲, △)

the layers. The transition temperatures are given in Table 2 for comparison with those obtained from specific heat data. A good agreement is observed between both field directions as well as between magnetic and specific heat data concerning the highest transition temperature. The remnant magnetisation does not fit a sum of two mean field type curves. There is a plateau at low temperature and at the transition it appears to be too sharp for a mean field type behaviour. Moreover for the $1/\chi$ *vs.* temperature curves, a smoother slope is observed below 100 K than between 100 and 300 K.

The hysteresis curves (induced magnetisation *vs.* magnetic field) were recorded at 4 K and are shown in Fig. 10. The values of the magnetisation at 17 000 Oe are nearly that expected (2.2 μ_B) for one Ni atom per formula unit. Depending on the direction of the applied field, different shapes are observed for the $M(H)$ curves. Remnant magnetisation is greater when H is applied perpendicular to the layers.

The coercive fields for both directions are linked in Table 3. They are of the same order of magnitude for samples 1 and 2 whatever the applied field direction. For sample 3 the coercive field is higher for H parallel to the layers than perpendicular.

Discussion and conclusion

We have synthesised 1:1 and 2:1 phyllosilicates in which octahedral sites are occupied by nickel. Three samples are reported: one representing a 1:1 and the other two belonging to the 2:1 phyllosilicate family. For one of them (sample 3) it was possible to expand the lattice to a 13.2 Å interlayer distance by means of the introduction of a diamine group substituting for an ethoxide group in TEOS. When a longer modifying group is used, a similar interlayer separation was observed. This result seems to indicate that the amine group is set parallel to the layer direction. However, it is not possible

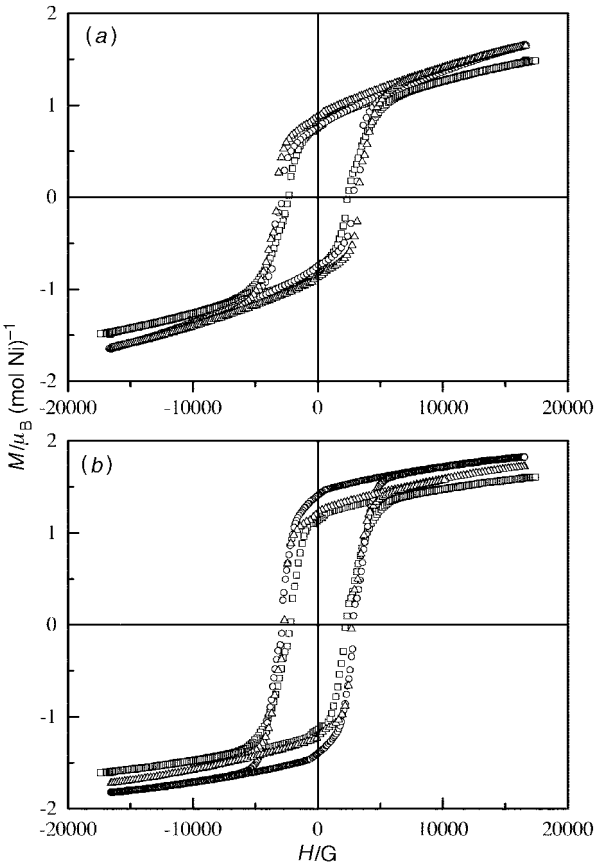

Fig. 10 Hysteresis cycles at 4 K for (*a*) *H* parallel and (*b*) *H* perpendicular to the layers of the structure for samples 1 (□), 2 (○) and 3 (△)

Table 3 Observed coercive fields at 4 K

sample	$H_\perp$/Oe	$H_\parallel$/Oe
1	2250	2380
2	2860	2860
3	2710	3240

to conclude whether the amine group is still bonded to Si or not.

In order to try to gain more insight into this behaviour, exchange experiments have been performed by dispersing the powder in a NaCl or KCl aqueous solution. The 2:1 structure is retained with different values for the (001) diffraction line even though a broadening of the diffraction lines was observed.

The fact that the diffraction peaks are relatively broad can be related to the small size of the particles. The Scherrer formula allows us to estimate their size as 3–6 nm for sample 3, *ca.* 10 nm for sample 2 and 15–20 nm for sample 1. Moreover, the unsymmetrical shape of some diffraction lines may be related to turbostratic disorder; such random stacking from one layer to another is often observed in clay related materials.[12] Comparing with the TEM results, rather good agreement is obtained for sample 1. For sample 2, the dimension calculated from XRD measurements corresponds to the smallest particles. For sample 3 which exhibits a fibrous aspect, the XRD value corresponds to the fibre diameter.

The thermal evolution revealed a higher stability for the 2:1 phyllosilicates compared to the 1:1 sample. Even for the expanded 2:1 sample, after pyrolysis of the diamine group, the 2:1 structure is retained at temperatures above 800 °C. The different thermal behaviours can be related to a possible stabilisation of OH groups sandwiched in between SiO_4 sheets in the 2:1 structure, whereas in the 1:1 structure most OH groups define an unshared plane of anions on the outer side of the octahedral sheet as depicted in Fig. 3. If the departure of an amine group non-bonded to Si appears easier without destroying the structure, the observation of a 2:1 structure after amine pyrolysis is again not proof for the possible location of the amine. Nevertheless it seems that its exchange by Na^+ or K^+ is possible; the exchange experiments resulting in an increase of the amount of adsorbed water, a shift of the thermal effect observed in the 300–400 °C range and a modification of the initial estimated molecular mass. All these facts could be related to an exchange reaction between amine groups and alkali metal ions. This exchange is only possible for amine groups not bonded to Si, *i.e.* for protonated amine groups inside the interlayer. However, the presence of a strong exotherm associated with CO_2 formation could indicate that either the exchange is not complete or that some of the amine groups are covalently bonded to Si. The observed increase of water desorption after treatment with Na^+ or K^+ solutions could be related to a partial exfoliation that will increase the available surface area.

The magnetic properties were explored in order to estimate the effect of the increasing distance between Ni layers, the experiments being performed using pellets to take into account the structural anisotropy. As previously described,[7,11] all compounds reveal ferromagnetic behaviour at low temperature. The hysteresis cycles show a larger magnetisation when *H* is perpendicular to the pellet and so it can be concluded that the easy magnetisation axis is perpendicular to the layers. It is noticeable that, for all samples, saturation is not reached even at 17 000 Oe. A theoretical value of 2.2 μ_B per mol (gS) is expected for Ni^{II}, while values of 1.61, 1.72 and 1.83 μ_B/mol Ni are measured for samples 1, 2 and 3, respectively, with *H* perpendicular to the pellets. This corresponds to 73, 78 and 83% saturation for the samples, respectively. The deviation is higher when the applied field direction is along the layers with values of 1.49 (68), 1.65 (75) and 1.64 (74%) μ_B/mol Ni, at 17 000 Oe. These results are in accord with previous experiments.[7,11] When the magnetic field is applied parallel to the layers, saturation is more difficult to achieve and is the reason why the cycles are more elongated and thus why the deviation from saturation increases at the same applied field of 17 000 Oe.

In the paramagnetic region, *g* values have been calculated and are in accord with expected values for Ni^{II}. For sample 1, the *g* value appears slightly higher than for the other two samples. This could be related to the participation of F^- ions in the Ni environment with the F^-/OH^- ratio being higher for the 1:1 sample compared to the 2:1 samples.

The rather high values of the coercive fields are also noticeable being close to 2500 Oe and not significantly depending on the applied field direction, except for sample 3. In the latter case, the variation of the coercive field with the applied field indicates that the anisotropy is more pronounced as the basal spacing increases. For 1:1 phyllosilicates, some authors[7,11] found that the coercive field was twice that (2100 Oe) than for 2:1 phyllosilicates (1050 Oe). Clearly the samples reported here exhibit coercive fields of the same order of magnitude. This can be attributed to the differences in the experimental conditions during the synthesis. This observation can also explain the difference in the transition temperatures.

A good agreement was found between the transition temperatures obtained by specific heat and remnant magnetisation. The slow decay of the remnant magnetisation to zero close to the transition temperature can be related to the existence of fluctuations. The two-step like curves could be related to a bimodal distribution in the crystallite size, especially for sample 2.

As pointed out by one of the referees, T_c depends on $J'S^2\xi^2$, where J' is the interplanar dipolar interaction, S the magnetic spin and ξ the correlation length. Considering that the materials have the same triangular arrangement but with increasing interplanar spacing we can follow the influence of changing J'

interaction on the transition temperatures. As the interlayer distance is increased, it is expected that a decrease in J' will result in a decrease of T_c when the intralayer interaction J remains constant. Transition temperatures (25, 29 and 27 K) are independent of the distance between adjacent NiO_6 layers [sample 1 (7 Å) to sample 2 (9.4 Å) and 3 (13.2 Å)]. This is not surprising because the effect on the transition temperature value of the interlayer interactions (dipolar origin) is very weak in comparison with the strong intralayer exchange interactions (indirect interactions through bridging anions).

These silicates present a Ni arrangement similar to that of $Ni(OH)_2$, in which the Ni···Ni interplanar distance is 4.6 Å, thus their magnetic behaviour can be compared. Nickel hydroxide is known to show three-dimensional antiferromagnetic order at low temperature. In this case, interplanar interactions are no longer negligible and occur *via* hydrogen bonds, leading to antiferromagnetic ordering. Moreover, it was shown that nickel hydroxynitrate in which d_{Ni-Ni} is 6.9 Å, displays a spin glass like behaviour at low temperature instead of three-dimensional antiferromagnetic ordering.[13] This compound also exhibits hydrogen bonds in the interlayered space but the NO_3^- disorder of NO_3^- groups implies spin glass behaviour. In our sample 1, a 7 Å distance between two adjacent NiO_6 layers also occurs but as no species could lead to hydrogen bonds from one layer to the other, the magnetic behaviour differs.

The authors wish to thank A. Derory and J.P. Lambour for magnetic measurements as well as M. Drillon and especially M. Kurmoo for helpful discussions.

References

1 J. S. Miller and A. J. Epstein, *Angew. Chem., Int Ed. Engl.*, 1994, **33**, 385.
2 D. Gatteschi, *Adv. Mater.*, 1994, **6**, 635.
3 O. Kahn, *Molecular Magnetism*, VCH, New York, 1993.
4 O. Kahn and Y. Journaux, in *Inorganic Materials*, ed. D. W. Bruce and D. O'Hare, Wiley, New York, 1993.
5 A. Abragam and B. Bleaney, *Electron Paramagnetic Resonance of Transition Metal Ions*, Clarendon Press, New York, 1970.
6 W. Reiff, B. C Dodrill and C. C. Torardi, *Mol. Cryst. Liq. Cryst.*, 1995, **274**, 137.
7 G. A. Martin, A. Renourez, G. Dalmai-Imelink and B. Imelink, *J. Chim. Phys.*, 1970, **67**, 1149.
8 C. S. Anderson and S. W. Bailey, *Am. Mineral.*, 1981, **66**, 185.
9 T. F. Semenova, I. V. Rozhdestvenskaya and V. A. Frank-Kamenetskii, *Kristallografiya*, 1977, **22**, 1196.
10 G. A. Martin and J. A. Dalmon, *C. R. Acad. Sci. Paris, Sér. B*, 1971, **272**, 304.
11 G. A. Martin, J. A. Dalmon, R. Dutartre, P. Turlier and J. C. Volta, *J. Chim. Phys.*, 1972, **2**, 277.
12 S. W. Bailey, *Rev. Mineral.*, 1988, **19**.
13 S. Rouba, Thesis of the Université Louis Pasteur de Strasbourg, 1996.

Paper 7/02985C; *Received* 1*st May*, 1997